communications physics

ARTICLE

https://doi.org/10.1038/s42005-023-01246-5 OPEN

Fractional magnetoresistance oscillations in spin-triplet superconducting rings

Gábor B. Halász [1]✉

Half-quantum vortices in spin-triplet superconductors are predicted to host Majorana zero modes and may provide a viable platform for topological quantum computation. Recent works also suggested that, in thin mesoscopic rings, the superconducting pairing symmetry can be probed via Little-Parks-like magnetoresistance oscillations of periodicity $\Phi_0 = h/2e$ that persist below the critical temperature. Here we use the London limit of Ginzburg-Landau theory to study these magnetoresistance oscillations resulting from thermal vortex tunneling in spin-triplet superconducting rings. For a range of temperatures in the presence of disorder, we find magnetoresistance oscillations with an emergent fractional periodicity Φ_0/n, where the integer $n \geq 3$ is entirely determined by the ratio of the spin and charge superfluid densities. These fractional oscillations can unambiguously confirm the spin-triplet nature of superconductivity and directly reveal the tunneling of half-quantum vortices in real-world candidate materials.

[1] Materials Science and Technology Division, Oak Ridge National Laboratory, Oak Ridge, TN 37831, USA. ✉email: halaszg@ornl.gov

Flux quantization is a defining feature of superconductivity that directly originates from the macroscopic quantum coherence of electron pairs. A salient manifestation of flux quantization (or more precisely, fluxoid quantization) is the Little-Parks effect[1] wherein the resistance of a hollow superconducting cylinder close to its critical temperature oscillates as a function of the magnetic flux inside with a periodicity given by the flux quantum $\Phi_0 = h/2e$. In thin mesoscopic rings where vortex-crossing processes lead to a finite resistance even in the superconducting state, analogous magnetoresistance oscillations with the same periodicity are also observable much below the critical temperature due to a periodic modulation of the vortex-crossing rate[2–5].

Recently, such magnetoresistance oscillations arising from both the conventional Little-Parks effect[6–9] and the rate of vortex crossings[10,11] have been identified as a useful tool in the ongoing search for exotic spin-triplet superconductors[12–19]. In addition to the standard quantum vortices corresponding to fluxoid quantization, these unconventional superconductors may also host half-quantum vortices around which the fluxoid is quantized to a half-integer multiple of Φ_0. With such half-quantum vortices present, the magnetoresistance oscillations are then expected to develop a characteristic two-peak structure[6,11,20]. Importantly, half-quantum vortices are also predicted to harbor Majorana zero modes[21,22] whose non-Abelian statistics may enable intrinsically fault-tolerant quantum computation[23,24].

In this work, we theoretically study the magnetoresistance oscillations in thin mesoscopic rings of spin-triplet superconductors below the critical temperature. Focusing on the London limit of Ginzburg-Landau theory, we adopt the formalism in ref. [25] to describe the available fluxoid states and thermal vortex-crossing processes by accounting for both the usual charge supercurrent and the spin supercurrent unique to spin-triplet superconductors. At the lowest temperatures, we verify that the magnetoresistance oscillates with periodicity Φ_0 and has a distinctive two-peak structure[6,11,20]. More interestingly, there is an intermediate temperature range in which disorder leads to magnetoresistance oscillations with a fractional periodicity Φ_0/n, where the integer $n \geq 3$ is determined by the ratio of the spin and charge superfluid densities[26]. Since these fractional oscillations directly reflect the enlarged number of available fluxoid states, we argue that they are defining hallmarks of spin-triplet superconductors supporting half-quantum vortices, much like the integer oscillations are for conventional spin-singlet superconductors.

Results and discussion

General formalism. We consider a circular superconducting ring of inner radius R_0 and outer radius ηR_0 in a perpendicular magnetic field $\vec{H} = H\vec{e}_z$ [see Fig. 1a]. We assume that the ring is made from a superconducting film of thickness $t \ll R_0$ and that the superconductor has spin-triplet $p_x + ip_y$ pairing with orbital angular momentum $m_l = +1$ with respect to the $\vec{e}_z$ direction. To allow for stable half-quantum vortices in the simplest possible setting, we also assume that spin-orbit coupling forces the spin pairing vector $\vec{d}$ into the plane perpendicular to $\vec{e}_z$ such that the spin angular momentum is restricted to $m_s = \pm 1$. The spin-triplet superconducting order parameter is then given by[26]

$$\hat{\Delta} = \begin{bmatrix} \Delta_{\uparrow\uparrow} & \Delta_{\uparrow\downarrow} \\ \Delta_{\downarrow\uparrow} & \Delta_{\downarrow\downarrow} \end{bmatrix} = \Delta_0 e^{i\chi} \begin{bmatrix} e^{i\alpha} & 0 \\ 0 & -e^{-i\alpha} \end{bmatrix}, \tag{1}$$

where χ is the usual superconducting phase corresponding to the overall charge supercurrent, while α corresponds to the difference between the spin-up ($\uparrow\uparrow$) and spin-down ($\downarrow\downarrow$) supercurrents, i.e., a pure spin supercurrent. In general, the central hole of the ring has a finite vorticity (fluxoid number) for each supercurrent such that χ (α) winds by $2\pi N_c$ ($2\pi N_s$) along the inner circumference of the ring. To understand how a vortex may travel across the ring, we further consider a vortex at position $\vec{r}_0 = (r_0, 0)$ inside the ring [see Fig. 1a] around which χ (α) winds by $2\pi n_c$ ($2\pi n_s$). Importantly, the order parameter is only single valued if the two numbers within each pair (N_c, N_s) and (n_c, n_s) are either both integer, corresponding to a standard quantum vortex, or both half integer, corresponding to a half-quantum vortex.

Assuming $R_0 \ll \Lambda$ with the Pearl length $\Lambda = 2\lambda^2/t$ and the penetration depth λ, the magnetic screening inside the superconductor is negligible, and the magnetic field $\vec{B}$ is identical to the external field $\vec{H}$[25]. In the London limit, corresponding to a small coherence length ξ, the magnitude Δ_0 of the order parameter at any position $\vec{r}$ further than ξ from $\vec{r}_0$ is constant, and the Ginzburg-Landau free energy is then[26]

$$F = \frac{t\Phi_0^2}{8\pi^2\mu_0\lambda^2} \int d^2\vec{r} \left[|\vec{J}_c|^2 + \gamma |\vec{J}_s|^2 \right] \tag{2}$$

in terms of the effective charge and spin supercurrents

$$\vec{J}_c = \vec{\nabla}\chi - \frac{2\pi}{\Phi_0}\vec{A}, \quad \vec{J}_s = \vec{\nabla}\alpha, \tag{3}$$

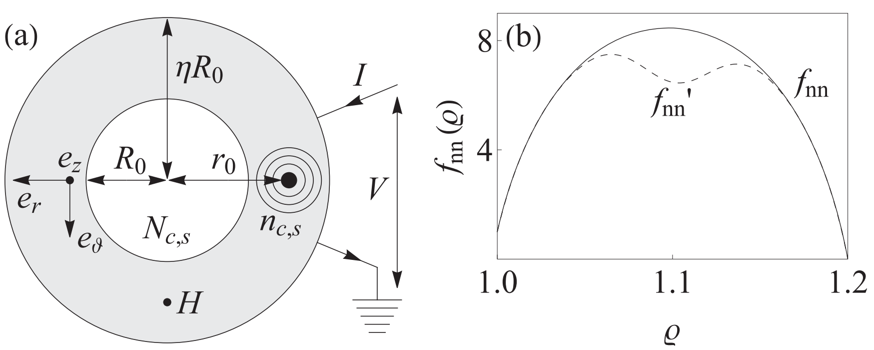

Fig. 1 General setup and definitions. a Thin-film superconducting ring with inner radius R_0 and outer radius ηR_0 in a perpendicular magnetic field $\vec{H} = H\vec{e}_z$. During a snapshot of a vortex-crossing process, the central hole of the ring has charge and spin vorticities (fluxoid numbers) $N_{c,s}$, while the vortex at radius r_0 inside the ring has charge and spin vorticities $n_{c,s}$. Experimentally, the resistance due to such vortex-crossing processes is found by applying a bias current I to a short section of the ring and measuring the voltage V between the two leads. **b** Vortex self energy $f_{nn}(\varrho)$ against the vortex position $\varrho = r_0/R_0$ for $\eta = 1.2$ without disorder (solid line) and with a single pinning site inside the ring (dashed line).

where the vector potential $\vec{A}$ satisfies $\vec{\nabla}\times\vec{A}=\vec{B}=\vec{H}$, while the ratio γ of the spin and charge superfluid densities[26] is expected to be smaller than 1 for interacting superconductors[27,28]. In the absence of a bias current I [see Fig. 1a], the charge supercurrent must satisfy the differential equations

$$\vec{\nabla}\cdot\vec{J}_c=0,\ \vec{\nabla}\times\vec{J}_c=\left[2\pi n_c\delta(\vec{r}-\vec{r}_0)-\frac{2h}{R_0^2}\right]\vec{e}_z \tag{4}$$

inside the superconductor, along with the boundary conditions

$$\vec{e}_n\cdot\vec{J}_c=0,\ \oint_{|\vec{r}|=R_0} d\vec{r}\cdot\vec{J}_c=2\pi(N_c-h) \tag{5}$$

at any interface with normal unit vector $\vec{e}_n$, and along the inner circumference of the ring, respectively, where $h=HR_0^2\pi/\Phi_0$ is a dimensionless external field. Importantly, the spin supercurrent $\vec{J}_s$ also satisfies Eqs. (4) and (5) with the substitutions $n_c\to n_s$, $N_c\to N_s$, and $h\to 0$. We further note that Eqs. (4) and (5) are equivalent to those studied in ref. [25].

Due to the linearity of Eqs. (4) and (5), the general solutions for the charge and spin supercurrents can be written as

$$\vec{J}_c=n_c\vec{J}_n+N_c\vec{J}_N-h\vec{J}_h,\ \vec{J}_s=n_s\vec{J}_n+N_s\vec{J}_N, \tag{6}$$

where $\vec{J}_n$, $\vec{J}_N$, and $\vec{J}_h$ are the particular solutions of Eqs. (4) and (5) with (n_c, N_c, h) being equal to $(1,0,0)$, $(0,1,0)$, and $(0,0,-1)$, respectively. Using polar coordinates, $\vec{r}=(r,\vartheta)$, one readily obtains $\vec{J}_N=(1/r)\vec{e}_\vartheta$ and $\vec{J}_h=(r/R_0^2)\vec{e}_\vartheta$, while $\vec{J}_n$ for a given vortex position $r_0=\varrho R_0$ was calculated in ref. [25]. Substituting Eq. (6) into Eq. (2), the free energy of the system in the pure (vortex-free) case with $n_{c,s}=0$ is then

$$F^{\rm pure}_{N_c,N_s,h}=F_0\left[f_{NN}\left(N_c^2+\gamma N_s^2\right)-2f_{Nh}N_ch+f_{hh}h^2\right], \tag{7}$$

while in the presence of a vortex at radius $r_0=\varrho R_0$ it reads

$$\begin{aligned}F^{\rm vortex}_{N_c,N_s,n_c,n_s,h}(\varrho)=F^{\rm pure}_{N_c,N_s,h}+F_0\big[f_{nn}(\varrho)\left(n_c^2+\gamma n_s^2\right)\\+2f_{nN}(\varrho)\left(n_cN_c+\gamma n_sN_s\right)-2f_{nh}(\varrho)\,n_ch\big],\end{aligned} \tag{8}$$

where $F_0=t\Phi_0^2\ln\eta/(4\pi\mu_0\lambda^2)$ is an overall energy scale, and $f_{XY}=(2\pi\ln\eta)^{-1}\int d^2\vec{r}\,\vec{J}_X\cdot\vec{J}_Y$ $(X,Y=n,N,h)$ are dimensionless free energies[25]:

$$\begin{aligned}&f_{NN}=1,\ f_{Nh}=\frac{\eta^2-1}{2\ln\eta},\ f_{hh}=\frac{\eta^4-1}{4\ln\eta},\\&f_{nN}(\varrho)=1-\frac{\ln\varrho}{\ln\eta},\ f_{nh}(\varrho)=\frac{\eta^2-\varrho^2}{2\ln\eta},\end{aligned} \tag{9}$$

while $f_{nn}(\varrho)$ has the form plotted in Fig. 1b. We remark that $f_{nn}(\varrho)$, corresponding to the self energy of the vortex, nominally diverges in the London limit and must be regularized with a small but finite coherence length ξ. We use $\xi/R_0\approx 0.02$ but emphasize that its precise value is not important as $f_{nn}(\varrho)$ is only logarithmically divergent.

Theory of magnetoresistance. We first assume that the superconducting ring in Fig. 1a is in thermal equilibrium without any bias current I. Because of the large vortex self energy in the London limit, there are no stable vortices inside the superconductor at sufficiently low temperatures. Nonetheless, at any finite temperature $T=1/\beta$, the fluxoid numbers $N_{c,s}$ of the central hole can thermally fluctuate, and the probability of the system to be in the fluxoid state (N_c,N_s) is given by

$$P_{(N_c,N_s)}=\frac{1}{Z}\exp\left[-\beta F^{\rm pure}_{N_c,N_s,h}\right], \tag{10}$$

where $Z=\sum_{N_c,N_s}\exp[-\beta F^{\rm pure}_{N_c,N_s,h}]$. The thermal fluctuations themselves happen by vortices traveling across the ring; the fluxoid state of the system transitions from (N_c,N_s) to (N_c',N_s') if a vortex with $(n_c,n_s)=\kappa(N_c'-N_c,N_s'-N_s)$ and $\kappa=+1$ $(\kappa=-1)$ crosses the ring in the inward (outward) direction. If these two processes are thermally activated, their respective free-energy barriers are[25]

$$\begin{aligned}F^{\rm barrier,+}_{(N_c,N_s)\to(N_c',N_s'),h}&=\max_\varrho F^{\rm vortex}_{N_c,N_s,N_c'-N_c,N_s'-N_s,h}(\varrho)-F^{\rm pure}_{N_c,N_s,h},\\F^{\rm barrier,-}_{(N_c,N_s)\to(N_c',N_s'),h}&=\max_\varrho F^{\rm vortex}_{N_c',N_s',N_c-N_c',N_s-N_s',h}(\varrho)-F^{\rm pure}_{N_c,N_s,h},\end{aligned} \tag{11}$$

and the total transition rate from (N_c,N_s) to (N_c',N_s') is then

$$\begin{aligned}\Gamma_{(N_c,N_s)\to(N_c',N_s'),h}&=P_{(N_c,N_s)}\,A_{(N_c,N_s)\to(N_c',N_s'),h},\\A_{(N_c,N_s)\to(N_c',N_s'),h}&\propto\sum_\pm\exp\left[-\beta F^{\rm barrier,\pm}_{(N_c,N_s)\to(N_c',N_s'),h}\right].\end{aligned} \tag{12}$$

We note that, in thermal equilibrium, detailed balance is satisfied: $\Gamma_{(N_c,N_s)\to(N_c',N_s'),h}=\Gamma_{(N_c',N_s')\to(N_c,N_s),h}$.

Next, we assume that a bias current I is applied by attaching two leads to the superconducting ring (see Fig. 1a). For each vortex with a given sign of the charge vorticity n_c, the bias current exerts a force in the inward or outward direction, thus leading to a net flow of such vortices in one of these directions by decreasing the free-energy barrier in one direction and increasing it in the other one. The resulting rate of phase slips then gives rise to a finite voltage between the two leads and translates into a finite resistance for the superconducting ring[29]. Without affecting our main results, we make a simplifying assumption that the two leads are close to each other along the ring (see Fig. 1a). In this case, the entire bias current goes through the short section of the ring between the two leads, and the probabilities $P_{(N_c,N_s)}$ of the fluxoid states are still given by Eq. (10). However, from the perspective of the transition rates $A_{(N_c,N_s)\to(N_c',N_s'),h}$ within the short section, the charge fluxoid number is effectively reduced by $\varepsilon=I/I_0$, where $I_0=t\Phi_0\ln\eta/(2\pi\mu_0\lambda^2)$. Hence, for a small bias current $I\ll I_0$, the resistance between the two leads becomes

$$R\propto\sum_{N_c,N_s}P_{(N_c,N_s)}\sum_{n_c,n_s}n_c\left.\frac{\partial A_{(N_c-\varepsilon,N_s)\to(\tilde{N}_c-\varepsilon,\tilde{N}_s),h}}{\partial\varepsilon}\right|_{\varepsilon=0}, \tag{13}$$

where $\tilde{N}_{c,s}\equiv N_{c,s}+n_{c,s}$, while $A_{(N_c-\varepsilon,N_s)\to(\tilde{N}_c-\varepsilon,\tilde{N}_s),h}$ for $\varepsilon\neq 0$ is computed through Eqs. (11) and (12) by formally evaluating Eqs. (7) and (8) at a fractional value of N_c. Finally, to obtain our full set of main results, we assume that the short section of the ring between the two leads contains some form of disorder. For concreteness, we first consider a single localized "pinning site" (e.g., defect or impurity) that renormalizes the vortex self energy from $f_{nn}(\varrho)$ to $f'_{nn}(\varrho)$ [see Fig. 1b], but later we also demonstrate that our main results are not sensitive to the precise form of disorder.

Fractional oscillations. The resistance R of the superconducting ring is plotted in Fig. 2 against the external field H for different values of the temperature T and the superfluid-density ratio γ. We parameterize the external field in terms of the dimensionless flux $\phi=\Phi/\Phi_0$, where $\Phi=HR_{\rm eff}^2\pi$ is the flux inside the effective mean radius[25]

$$R_{\rm eff}=R_0\sqrt{\frac{f_{Nh}}{f_{NN}}}=R_0\sqrt{\frac{\eta^2-1}{2\ln\eta}}. \tag{14}$$

In this parameterization, conventional magnetoresistance oscillations in spin-singlet superconductors[2–5] have unit periodicity $\Delta\phi=1$ with a peak at each external field $\phi=N+1/2$ $(N\in\mathbb{Z})$ as explicitly confirmed in Supplementary Note 1. In

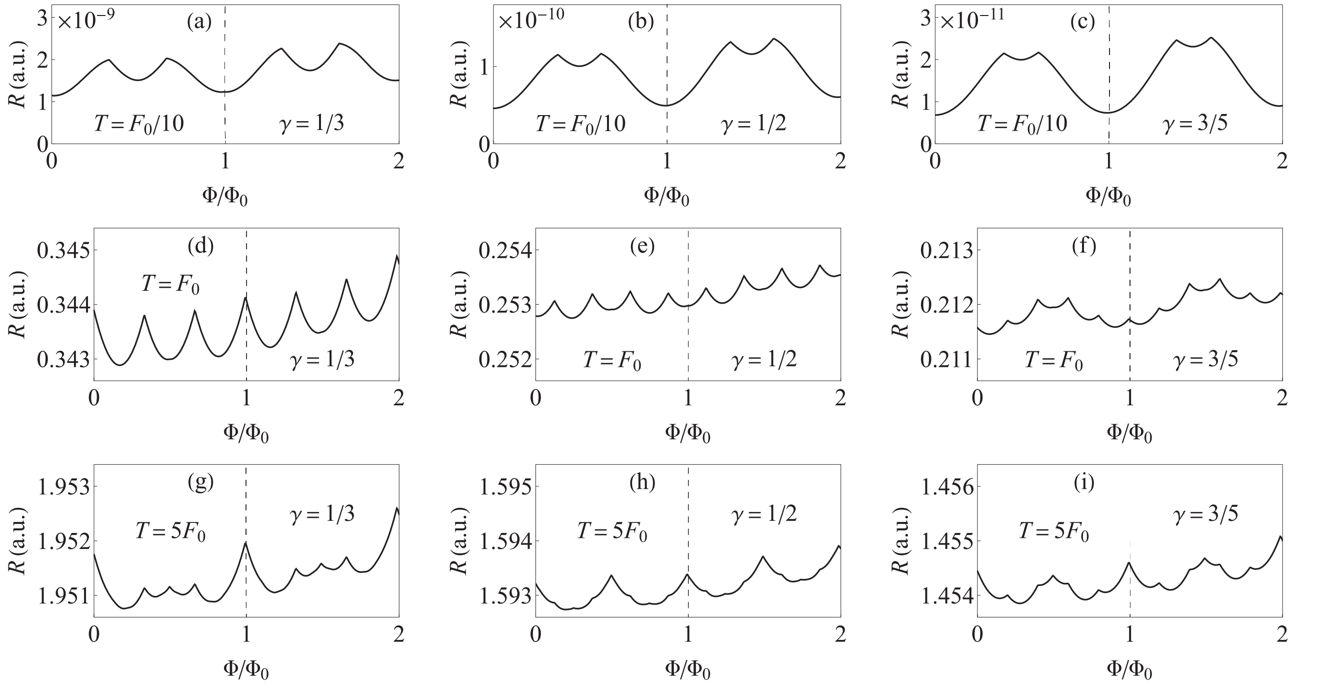

Fig. 2 Magnetoresistance oscillations at different temperatures. Resistance R of the superconducting ring in Fig. 1a, as calculated from Eq. (13), against the dimensionless flux $\phi = \Phi/\Phi_0$ at low temperatures $T = F_0/10$ (**a**–**c**), intermediate temperatures $T = F_0$ (**d**–**f**), and high temperatures $T = 5F_0$ (**g**–**i**) [in terms of $F_0 = t\Phi_0^2 \ln \eta/(4\pi\mu_0\lambda^2)$] for a radius ratio $\eta = 1.2$ and superfluid-density ratios $\gamma = 1/3$ (**a**, **d**, **g**), $\gamma = 1/2$ (**b**, **e**, **h**), and $\gamma = 3/5$ (**c**, **f**, **i**) in the presence of a single pinning site inside the ring [see Fig. 1b].

contrast, Fig. 2 shows that spin-triplet superconductors with $\gamma < 1$ possess nontrivial additional structure in their magnetoresistance oscillations. For the lowest temperatures ($T \ll F_0$), the periodicity is still $\Delta\phi = 1$, but each peak at $\phi = N + 1/2$ splits into two peaks that move further apart as γ is decreased[6,11,20]. For high temperatures ($T \gg F_0$), the oscillations are significantly more complex with an overall periodicity $\Delta\phi = 1$ or $\Delta\phi = 1/2$. Most interestingly, for intermediate temperatures ($T \sim F_0$), the magnetoresistance oscillations have an emergent fractional periodicity $\Delta\phi = 1/n$, where the integer n is determined by the superfluid-density ratio γ. While Fig. 2 suggests that the different integers $n \geq 3$ correspond to specific rational values of γ, it is demonstrated in Figs. 3 and 4 that the fractional periodicities $\Delta\phi = 1/n$ persist in finite ranges of both γ and T. In particular, the Fourier analysis of the oscillation components in Fig. 4 reveals that the fractional periodicities $\Delta\phi = 1/3$, $\Delta\phi = 1/4$, and $\Delta\phi = 1/5$ are observable for $0.25 \lesssim \gamma \lesssim 0.45$, $0.45 \lesssim \gamma \lesssim 0.55$, and $0.55 \lesssim \gamma \lesssim 0.65$, respectively.

To understand these fractional oscillations, we first notice that the free energy of a pure (vortex-free) system in Eq. (7) can be written in the new parameterization as

$$F^{\text{pure}}_{N_c,N_s,\phi} = F_0\left[\left(N_c - \phi\right)^2 + \gamma N_s^2 + g(\phi)\right]. \tag{15}$$

For external field ϕ, the free-energy difference between two fluxoid states (N_c, N_s) and $(\tilde{N}_c, \tilde{N}_s) = (N_c + n_c, N_s + n_s)$, connected by vortices $\pm(n_c, n_s)$ crossing the ring, is then

$$\begin{aligned} F^{\text{pure}}_{\tilde{N}_c,\tilde{N}_s,\phi} - F^{\text{pure}}_{N_c,N_s,\phi} = {} & 2F_0\left[n_c\left(N_c - \phi\right) + \gamma n_s N_s\right] \\ & + F_0\left(n_c^2 + \gamma n_s^2\right). \end{aligned} \tag{16}$$

Moreover, if the radius ratio η of the superconducting ring is not too large, $f_{nN}(\varrho)$ and $f_{nh}(\varrho)$ in Eq. (9) are close to linear for $1 \leq \varrho \leq \eta$. Hence, taking a linear interpolation between their values at $\varrho = 1$ and $\varrho = \eta$, the free energy of the system with a single vortex (see Eq. (8)) can be approximated by

$$\begin{aligned} F^{\text{vortex}}_{N_c,N_s,n_c,n_s,\phi}(\varrho) = {} & F^{\text{pure}}_{N_c,N_s,\phi} + F_0 f'_{nn}(\varrho)\left(n_c^2 + \gamma n_s^2\right) \\ & + 2F_0\left[n_c\left(N_c - \phi\right) + \gamma n_s N_s\right]\frac{\eta - \varrho}{\eta - 1}. \end{aligned} \tag{17}$$

Importantly, if we use this approximation, the transition rates $A_{(N_c,N_s)\to(N_c+n_c,N_s+n_s),\phi}$ in Eq. (12) only depend on either ϕ or $N_{c,s}$ via the combination $n_c(N_c - \phi) + \gamma n_s N_s$, and the resistance in Eq. (13) thus takes the general form

$$R \propto \sum_{N_c,N_s} P_{(N_c,N_s)} \sum_{n_c,n_s} G_{n_c,n_s}\left[n_c\left(N_c - \phi\right) + \gamma n_s N_s\right]. \tag{18}$$

Due to the many identical contributions G_{n_c,n_s} corresponding to different $N_{c,s}$, each shifted by $N_c + \gamma N_s n_s/n_c$ in the field ϕ, this form naturally leads to periodic oscillations.

Next, we recall from Eq. (17) that the vortex self energy is proportional to $n_c^2 + \gamma n_s^2$. For any $\gamma < 1$, the dominant vortices contributing to the resistance at sufficiently low temperatures $[T \ll F_0 \max_\varrho f'_{nn}(\varrho)]$ are then the half-quantum vortices with $n_{c,s} = \pm 1/2$. In the intermediate temperature range ($T \sim F_0$), there are also many fluxoid states (N_c, N_s) with sizeable probabilities $P_{(N_c,N_s)} \sim 1$. If we then sum over the identical contributions $G_{\pm 1/2,\pm 1/2}$ in Eq. (18) for all possible $N_{c,s}$, each shifted by $N_c \pm \gamma N_s$ in the field ϕ, these identical contributions conspire to produce fractional oscillations with periodicity $\Delta\phi = 1/n$. For a rational value of the superfluid-density ratio, $\gamma = p/q$, with the integers p and q being relative primes, it is shown in Supplementary Note 2 that $n = q$ if p and q are both odd and $n = 2q$ otherwise. Therefore, in accordance with Fig. 2, the fractional periodicities are $\Delta\phi = 1/3$, $\Delta\phi = 1/4$, and $\Delta\phi = 1/5$ for $\gamma = 1/3$, $\gamma = 1/2$, and $\gamma = 3/5$, respectively. In practice, since the summation over $N_{c,s}$ is cut off at any finite temperature $T \sim F_0$, only the fractional periodicities with small p and q are observable, but each of them remains observable in a finite range around $\gamma = p/q$ (see Figs. 3 and 4). As an interesting aside, we point out that the

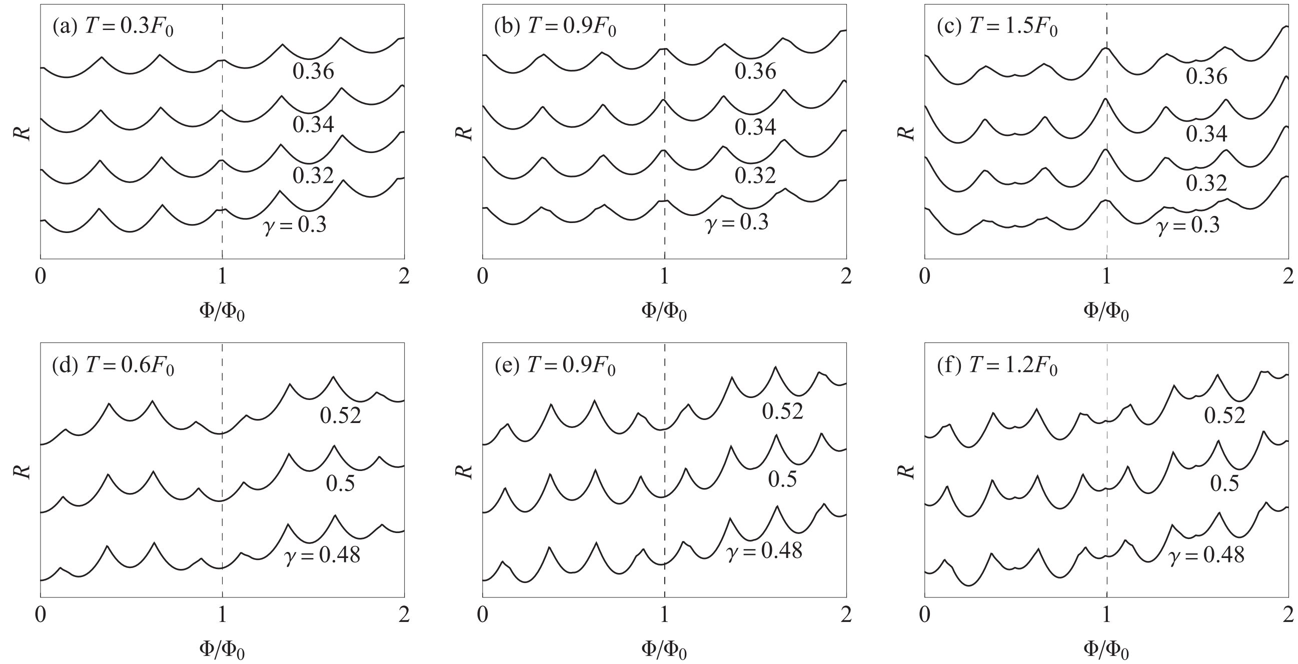

Fig. 3 Robustness of fractional oscillations. Magnetoresistance oscillations with fractional periodicities $\Delta\phi = 1/3$ (**a**–**c**) and $\Delta\phi = 1/4$ (**d**–**f**) in the intermediate temperature ranges $0.3 \le T/F_0 \le 1.5$ and $0.6 \le T/F_0 \le 1.2$ for superfluid-density ratios $0.3 \le \gamma \le 0.36$ and $0.48 \le \gamma \le 0.52$, respectively. In each case, the resistance R of the superconducting ring in Fig. 1a is calculated from Eq. (13) against the dimensionless flux $\phi = \Phi/\Phi_0$ for a radius ratio $\eta = 1.2$ in the presence of a single pinning site inside the ring [see Fig. 1b]. The different curves are labeled by γ and are vertically shifted with respect to each other for better visibility.

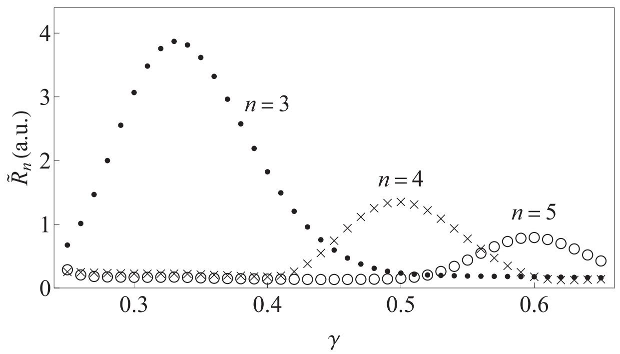

Fig. 4 Robustness of fractional periodicities. Fourier amplitudes $\tilde{R}_n \propto |\int_0^1 d\phi\, R(\phi)\, e^{2\pi i n\phi}|$ of the magnetoresistance components corresponding to the fractional periodicities $\Delta\phi = 1/n$ with $n = 3$ (dots), $n = 4$ (crosses), and $n = 5$ (circles) against the superfluid-density ratio γ at the intermediate temperature $T = F_0$. For each γ, the magnetoresistance $R(\phi)$ of the superconducting ring in Fig. 1a is calculated from Eq. (13) for a radius ratio $\eta = 1.2$ in the presence of a single pinning site inside the ring [see Fig. 1b].

emergence of fractional oscillations and the intimate connection between $\Delta\phi$ and γ can also be understood from the simple geometric picture presented in Fig. 5.

We finally remark that, as the temperature T approaches the critical temperature of the superconductor, the effective temperature T/F_0 with $F_0 = t\Phi_0^2 \ln\eta/(4\pi\mu_0\lambda^2)$ diverges as a result of $\lambda \to \infty$. Therefore, in principle, the intermediate temperatures $T \sim F_0$ that give rise to the fractional magnetoresistance oscillations are attainable for any ring dimensions. In practice, however, we expect the fractional oscillations to be more observable further away from the critical temperature, which is achieved by keeping both the film thickness t and the radius ratio η as small as possible.

Effect of disorder. Remarkably, the fractional magnetoresistance oscillations only emerge if disorder is present in the superconductor. This property is demonstrated in Fig. 6 where the magnetoresistance is plotted without any disorder and with different kinds of disorder: a single pinning site [see Fig. 1b] of two different depths, a collection of three pinning sites, and a random potential landscape (i.e., extended disorder). While the magnetoresistance is completely featureless in the absence of disorder, it exhibits fractional oscillations with the same periodicity if any kind of disorder is included.

Indeed, even though the fractional periodicity $\Delta\phi = 1/n$ is a robust emergent feature connected to the superfluid-density ratio γ, the corresponding oscillations are not observable if the functions $G_{\pm 1/2, \pm 1/2}$ are completely smooth. The crucial role of disorder is to produce nonanalytic features in $G_{\pm 1/2, \pm 1/2}$ that can be replicated with periodicity $\Delta\phi$ as a function of the field ϕ. In the following, we restrict our attention to a single pinning site (see Fig. 1b) and describe how it gives nonanalytic features (cusps) in the transition rate $A_{(0,0)\to(1/2,1/2),\phi}$ (see Eq. (12)) and hence the function $G_{1/2,1/2}$ that manifest as sharp peaks in the magnetoresistance.

From Eq. (12), the transition rate $A_{(0,0)\to(1/2,1/2),\phi}$ at any given temperature only depends on the two vortex-crossing barriers $F^{\text{barrier},\pm}_{(0,0)\to(1/2,1/2),\phi}$. The inward vortex-crossing barrier $F^{\text{barrier},+}_{(0,0)\to(1/2,1/2),\phi}$ is plotted in Fig. 7a against the field ϕ and shows a clear cusp at a critical field ϕ_0^+. Noting that the vortex-crossing barrier $F^{\text{barrier},+}_{(0,0)\to(1/2,1/2),\phi}$ is determined by the maximum of the vortex energy function $F^{\text{vortex}}_{0,0,1/2,1/2,\phi}(\varrho)$ in the vortex position ϱ (see Eq. (11)), it is then illustrated in Fig. 7b-d that the critical field ϕ_0^+ corresponds to a discontinuity in the vortex position ϱ_0^+ that maximizes the vortex energy function $F^{\text{vortex}}_{0,0,1/2,1/2,\phi}(\varrho)$. Analogously, the outward vortex-crossing barrier $F^{\text{barrier},-}_{(0,0)\to(1/2,1/2),\phi}$ has a cusp at another critical field ϕ_0^- corresponding to a discontinuity in the

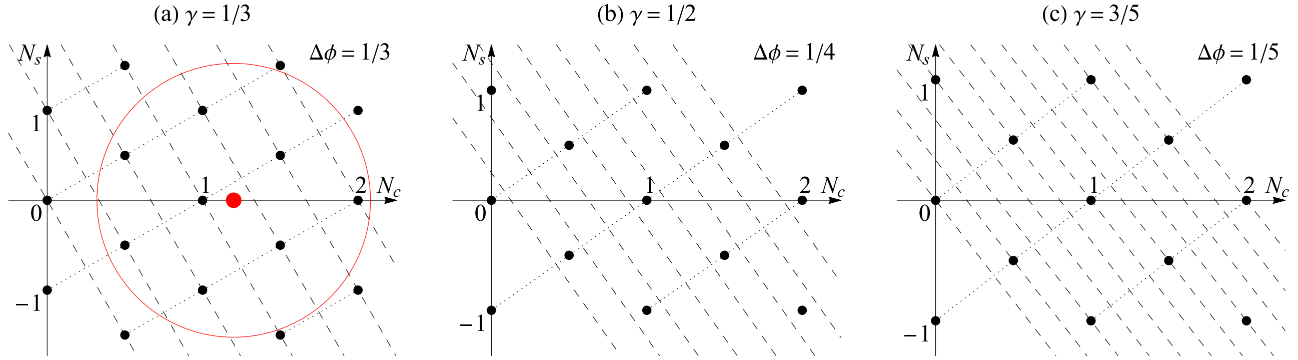

Fig. 5 Geometric interpretation of fractional oscillations. Emergence of the fractional periodicities $\Delta\phi = 1/3$ (**a**), $\Delta\phi = 1/4$ (**b**), and $\Delta\phi = 1/5$ (**c**) from the superfluid-density ratios $\gamma = 1/3$, $\gamma = 1/2$, and $\gamma = 3/5$, respectively. Within a two-dimensional plane, the black dots depict the possible fluxoid states (N_c, N_s), while the red dot at position $(\phi, 0)$ represents the external field. Due to the scaling factor $\sqrt{\gamma}$ between the vertical (N_s) and horizontal (N_c) dimensions, the energy of a given fluxoid state is proportional to the distance squared between the corresponding black dot and the red dot [see Eq. (15)]. Focusing on the half-quantum transitions $n_{c,s} = \Delta N_{c,s} = 1/2$ (dotted lines), the argument $(N_c + \gamma N_s - \phi)/2$ of $G_{1/2,1/2}$ in Eq. (18) corresponds to the perpendicular projection of the red dot onto the dotted line connecting (N_c, N_s) and $(N_c + 1/2, N_s + 1/2)$. Therefore, as the external field ϕ is increased, the same feature in the magnetoresistance is periodically replicated every time the red dot at position $(\phi, 0)$ crosses a perpendicular bisector (dashed line). Relevant transitions connecting fluxoid states with sizeable probabilities are within the red circle whose radius scales with the square root of the temperature.

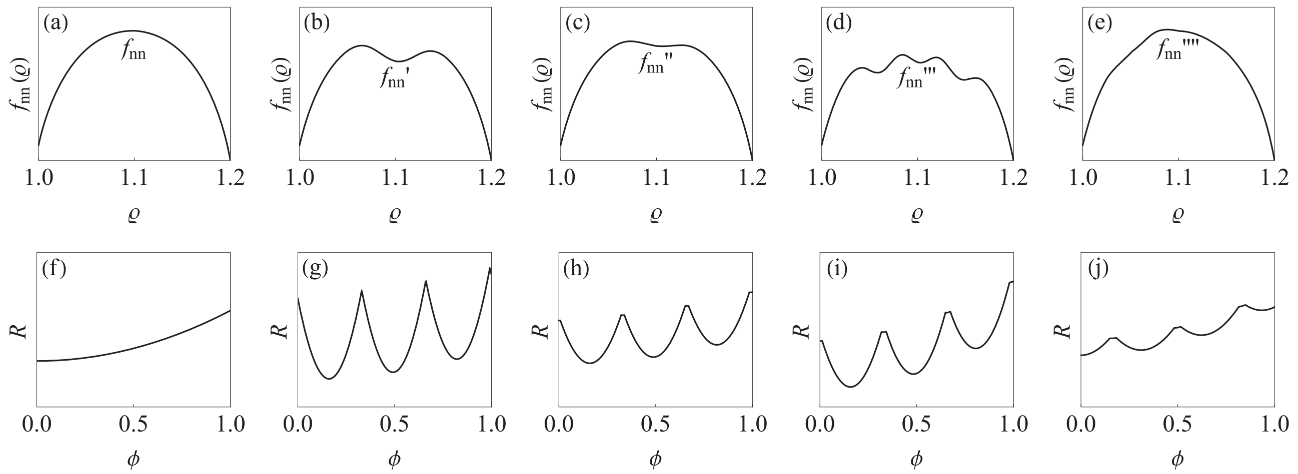

Fig. 6 Relation between disorder and fractional oscillations. Vortex self energy $f_{nn}(\varrho)$ against the dimensionless vortex position ϱ (**a–e**) and the corresponding resistance R of the superconducting ring in Fig. 1a against the external field (i.e., dimensionless flux) $\phi = \Phi/\Phi_0$ at the intermediate temperature $T = F_0/2$ (**f–j**) for a radius ratio $\eta = 1.2$ and a superfluid-density ratio $\gamma = 1/3$ without any disorder (**a**, **f**), with a single pinning site of a larger depth (**b**, **g**) and a smaller depth (**c**, **h**), with a collection of three pinning sites (**d**, **i**), and with a random potential landscape (**e**, **j**).

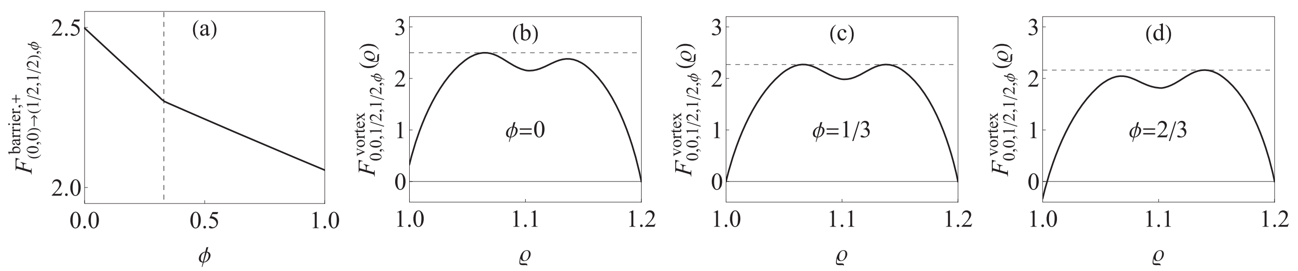

Fig. 7 Connection between disorder and vortex-crossing barriers. a Vortex-crossing barrier $F^{\mathrm{barrier},+}_{(0,0)\to(1/2,1/2),\phi}$ against the external field $\phi = \Phi/\Phi_0$ for a radius ratio $\eta = 1.2$ and a superfluid-density ratio $\gamma = 1/3$ with a single pinning site inside the ring [see Fig. 1b]. The dashed line indicates the critical field $\phi_0^+ \approx 1/3$ at which the first derivative has a discontinuity. **b–d** Vortex energy function $F^{\mathrm{vortex}}_{0,0,1/2,1/2,\phi}(\varrho)$ against the dimensionless vortex position ϱ for three different external fields: $\phi = 0$ (**b**), $\phi = 1/3$ (**c**), and $\phi = 2/3$ (**d**). In each case, the dashed line marks the maximum of the vortex energy function, i.e., the vortex-crossing barrier in subfigure **a**. The critical field $\phi_0^+ \approx 1/3$ corresponds to a discontinuity in the vortex position ϱ_0^+ that maximizes the vortex energy function.

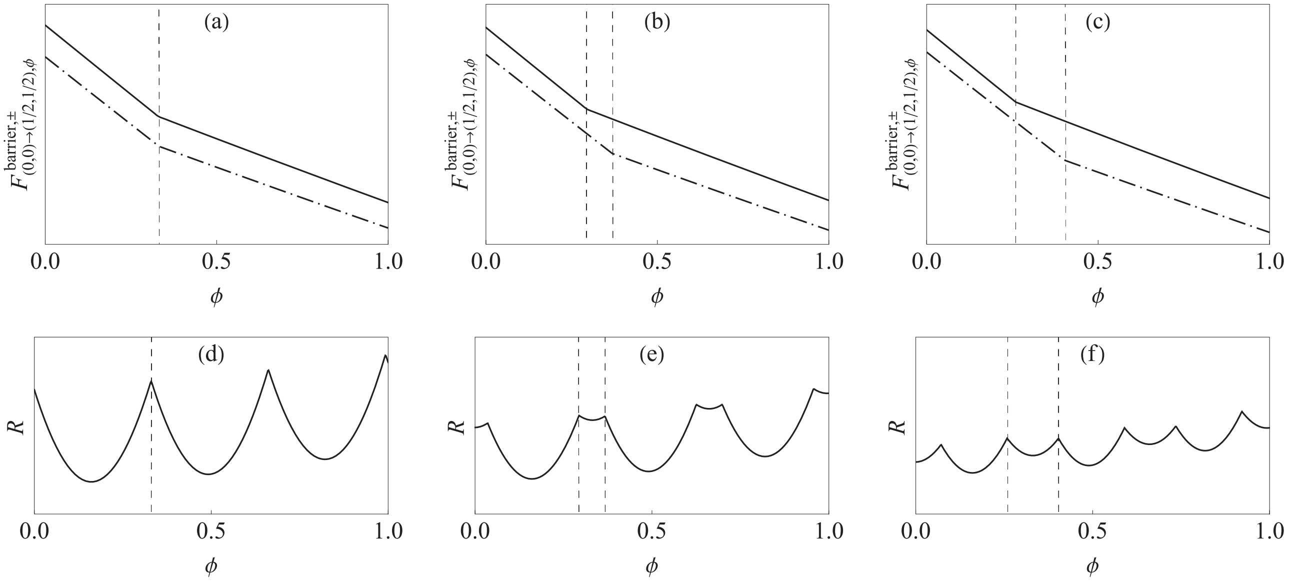

Fig. 8 Connection between vortex-crossing barriers and magnetoresistance peaks. Vortex-crossing barriers $F^{\mathrm{barrier},\pm}_{(0,0)\to(1/2,1/2),\phi}$ (**a**–**c**) and the corresponding resistance R of the superconducting ring at the intermediate temperature $T = F_0/2$ (**d**–**f**) against the external field $\phi = \Phi/\Phi_0$ for a radius ratio $\eta = 1.2$ and a superfluid-density ratio $\gamma = 1/3$ with a single pinning site at (**a**, **d**) the same location as in Fig. 1b and (**b**, **c**, **e**, **f**) moved in the inward direction by a smaller amount (**b**, **e**) and a larger amount (**c**, **f**). The two vortex-crossing barriers $F^{\mathrm{barrier},+}_{(0,0)\to(1/2,1/2),\phi}$ (solid line) and $F^{\mathrm{barrier},-}_{(0,0)\to(1/2,1/2),\phi}$ (dash-dotted line) are vertically shifted with respect to each other for better visibility. In each case, the dashed lines indicate the two critical fields $\phi_0^{\pm}$ that correspond to cusps in the vortex-crossing barriers and peaks replicated with periodicity $\Delta\phi = 1/3$ in the magnetoresistance.

vortex position ϱ_0^- that maximizes the vortex energy function $F^{\mathrm{vortex}}_{1/2,1/2,-1/2,-1/2,\phi}(\varrho)$ (see Eq. (11)).

For the particular location of the pinning site in Fig. 1b, the two vortex-crossing barriers have identical critical fields: $\phi_0^+ = \phi_0^-$ (see Fig. 8a). If the pinning site is moved inward or outward, the two critical fields $\phi_0^{\pm}$ then shift in opposite directions and are generically different (see Fig. 8b, c). Consequently, the fractional magnetoresistance oscillations may develop a two-peak structure while retaining the same fractional periodicity (see Fig. 8d–f). For more general disorder, we expect multiple features (not necessarily peaks) in the magnetoresistance that are all replicated with the given periodicity $\Delta\phi$. While the precise shape and amplitude of the fractional oscillations thus depends on the specific form of disorder, the fractional periodicity $\Delta\phi$ is universal and only depends on the superfluid-density ratio γ (see Fig. 6).

Data availability

The data that support the findings of this study are available from the author upon reasonable request.

Code availability

The codes that support the findings of this study are available from the author upon reasonable request.

Received: 13 April 2023; Accepted: 22 May 2023;
Published online: 09 June 2023

References

1. Little, W. A. & Parks, R. D. Observation of quantum periodicity in the transition temperature of a superconducting cylinder. *Phys. Rev. Lett.* **9**, 9 (1962).
2. Sochnikov, I., Shaulov, A., Yeshurun, Y., Logvenov, G. & Božović, I. Large oscillations of the magnetoresistance in nanopatterned high-temperature superconducting films. *Nat. Nanotechnol.* **5**, 516 (2010).
3. Sochnikov, I., Shaulov, A., Yeshurun, Y., Logvenov, G. & Božović, I. Oscillatory magnetoresistance in nanopatterned superconducting $La_{1.84}$ $Sr_{0.16}$ CuO_4 films. *Phys. Rev. B* **82**, 094513 (2010).
4. Berdiyorov, G. R. et al. Large magnetoresistance oscillations in mesoscopic superconductors due to current-excited moving vortices. *Phys. Rev. Lett.* **109**, 057004 (2012).
5. Mills, S. A., Shen, C., Xu, Z. & Liu, Y. Vortex crossing and trapping in doubly connected mesoscopic loops of a single-crystal type-II superconductor. *Phys. Rev. B* **92**, 144502 (2015).
6. Yasui, Y. et al. Little-Parks oscillations with half-quantum fluxoid features in Sr_2 RuO_4 microrings. *Phys. Rev. B* **96**, 180507(R) (2017).
7. Li, Y., Xu, X., Lee, M.-H., Chu, M.-W. & Chien, C. L. Observation of half-quantum flux in the unconventional superconductor β -Bi_2 Pd. *Science* **366**, 238 (2019).
8. Xu, X., Li, Y. & Chien, C. L. Spin-triplet pairing state evidenced by half-quantum flux in a noncentrosymmetric superconductor. *Phys. Rev. Lett.* **124**, 167001 (2020).
9. Li, Y., Xu, X., Lee, S.-P. & Chien, C. L. Fractional Little-Parks effect observed in a topological superconductor. *arXiv* https://doi.org/10.48550/arXiv.2003.00603 (2020).
10. Cai, X. et al. Unconventional quantum oscillations in mesoscopic rings of spin-triplet superconductor Sr_2 RuO_4. *Phys. Rev. B* **87**, 081104(R) (2013).
11. Cai, X. et al. Magnetoresistance oscillation study of the spin counterflow half-quantum vortex in doubly connected mesoscopic superconducting cylinders of Sr_2 RuO_4. *Phys. Rev. B* **105**, 224510 (2022).
12. Maeno, Y. et al. Superconductivity in a layered perovskite without copper. *Nature* **372**, 532 (1994).
13. Maeno, Y., Rice, T. M. & Sigrist, M. The intriguing superconductivity of strontium ruthenate. *Phys. Today* **54**, 42 (2001).
14. Mackenzie, A. P. & Maeno, Y. The superconductivity of Sr_2 RuO_4 and the physics of spin-triplet pairing. *Rev. Mod. Phys.* **75**, 657 (2003).
15. Maeno, Y., Kittaka, S., Nomura, T., Yonezawa, S. & Ishida, K. Evaluation of Spin-Triplet Superconductivity in Sr_2 RuO_4. *J. Phys. Soc. Jpn* **81**, 011009 (2012).
16. Kallin, C. Chiral p-wave order in Sr_2 RuO_4. *Rep. Prog. Phys.* **75**, 042501 (2012).
17. Mackenzie, A. P., Scaffidi, T., Hicks, C. W. & Maeno, Y. Even odder after twenty-three years: the superconducting order parameter puzzle of Sr_2 RuO_4. *npj Quant. Mater.* **2**, 40 (2017).
18. Ran, S. et al. Nearly ferromagnetic spin-triplet superconductivity. *Science* **365**, 684 (2019).
19. Aoki, D. et al. Unconventional superconductivity in UTe_2. *J. Phys. Condens. Matter* **34**, 243002 (2022).
20. Vakaryuk, V. & Vinokur, V. Effect of half-quantum vortices on magnetoresistance of perforated superconducting films. *Phys. Rev. Lett.* **107**, 037003 (2011).

21. Ivanov, D. A. Non-abelian statistics of half-quantum vortices in p-wave superconductors. *Phys. Rev. Lett.* **86**, 268 (2001).
22. Alicea, J. New directions in the pursuit of Majorana fermions in solid state systems. *Rep. Prog. Phys.* **75**, 076501 (2012).
23. Kitaev, A. Y. Fault-tolerant quantum computation by anyons. *Ann. Phys.* **303**, 2 (2003).
24. Nayak, C., Simon, S. H., Stern, A., Freedman, M. & Das Sarma, S. Non-Abelian anyons and topological quantum computation. *Rev. Mod. Phys.* **80**, 1083 (2008).
25. Kogan, V. G., Clem, J. R. & Mints, R. G. Properties of mesoscopic superconducting thin-film rings: London approach. *Phys. Rev. B* **69**, 064516 (2004).
26. Chung, S. B., Bluhm, H. & Kim, E.-A. Stability of half-quantum vortices in p_x+ip_y superconductors. *Phys. Rev. Lett.* **99**, 197002 (2007).
27. Leggett, A. J. Inequalities, instabilities, and renormalization in metals and other fermi liquids. *Ann. Phys.* **46**, 76 (1968).
28. Leggett, A. J. A theoretical description of the new phases of liquid ^{3}He. *Rev. Mod. Phys.* **47**, 331 (1975).
29. Halperin, B. I., Refael, G. & Demler, E. Resistance in superconductors. *Int. J. Mod. Phys. B* **24**, 4039 (2010).

Acknowledgements

We thank Benjamin Lawrie and Yun-Yi Pai for experimental motivation as well as Eugene Dumitrescu and Chengyun Hua for helpful discussions. This research was sponsored by the U. S. Department of Energy, Office of Science, Basic Energy Sciences, Materials Sciences and Engineering Division. This manuscript has been authored by UT-Battelle, LLC under Contract No. DE-AC05-00OR22725 with the U.S. Department of Energy. The United States Government retains and the publisher, by accepting the article for publication, acknowledges that the United States Government retains a non-exclusive, paid-up, irrevocable, world-wide license to publish or reproduce the published form of this manuscript, or allow others to do so, for United States Government purposes. The Department of Energy will provide public access to these results of federally sponsored research in accordance with the DOE Public Access Plan (http://energy.gov/downloads/doe-public-access-plan).

Author contributions

G.B.H. designed the study, performed the calculations, and wrote the manuscript.

Competing interests

The author declares no competing interests.

Additional information

Supplementary information The online version contains supplementary material available at https://doi.org/10.1038/s42005-023-01246-5.

Correspondence and requests for materials should be addressed to Gábor B. Halász.

Peer review information *Communications Physics* thanks the anonymous reviewers for their contribution to the peer review of this work.

Reprints and permission information is available at http://www.nature.com/reprints

Publisher's note Springer Nature remains neutral with regard to jurisdictional claims in published maps and institutional affiliations.

Open Access This article is licensed under a Creative Commons Attribution 4.0 International License, which permits use, sharing, adaptation, distribution and reproduction in any medium or format, as long as you give appropriate credit to the original author(s) and the source, provide a link to the Creative Commons license, and indicate if changes were made. The images or other third party material in this article are included in the article's Creative Commons license, unless indicated otherwise in a credit line to the material. If material is not included in the article's Creative Commons license and your intended use is not permitted by statutory regulation or exceeds the permitted use, you will need to obtain permission directly from the copyright holder. To view a copy of this license, visit http://creativecommons.org/licenses/by/4.0/.

© The Author(s) 2023